ELSEVIER

Polymer 41 (2000) 3751–3758

polymer

Structure of isotactic polypropylene–hydrogenated oligo(cyclopentadiene) (iPP–HOCP) blends Part II. HOCP-rich blends

A. Triolo[a,*], J.S. Lin[b], G.D. Wignall[b], R. Triolo[c]

[a]*Department of Chemistry, Heriot-Watt University, Edinburgh EH14 4AS, UK*
[b]*Solid State Division, Oak Ridge National Laboratory, Oak Ridge, TN 37831, USA*
[c]*Dipartimento di Chimica Fisica, Università di Palermo, Parco d'Orleans II, 90128 Palermo, Italy*

Received 1 January 1999; received in revised form 10 May 1999; accepted 25 May 1999

Abstract

Blends of isotactic polypropylene (iPP) and hydrogenated oligo(cyclopentadiene) (HOCP) were investigated to gain structural information by means of both SAXS and SANS techniques. The composition range (from 30 to 60% w/w HOCP content) and the temperature range (between 25 and 160°C) were chosen in order to cover the miscibility gap in the phase diagram of the material system.

In a previous report, blends lying outside the miscibility gap have been investigated and the corresponding SAXS patterns were interpreted in terms of a pseudo-two phase model. For the SAXS patterns, blends lying inside the miscibility gap are rather hard to be interpreted in terms of such a model. On the other hand, SANS patterns display a behaviour that can be directly rationalised in terms of two different coexisting lamellar phases (each corresponding to two domains enriched in either one of the two components). A novel approach is described which allows such a separation of morphological phases.

Keywords: SAXS; SANS; iPP

1. Introduction

In the last decade, a great deal of interest and numerous studies have been devoted to the blending of iPP with HOCP, because of the particular enhancement of some technological properties of iPP, after blending. One of the most interesting applications of iPP–HOCP blends is in the packaging industry, primarily due to the reduced permeability to oxygen and aromas of these blends.

The scientific interest in these blends has increased progressively, and in the last years some experimental results indicated a number of peculiar yet interesting properties. First results referred to mechanical, thermal and morphological properties [1,2]. More recently, we have analysed the results of small-angle X-ray scattering (SAXS) in the study of structural properties of iPP-rich blends [3,4], which show a lamellar morphology where crystalline iPP layers alternate with amorphous iPP and HOCP layers, and HOCP is the non-crystallizable component. Our analysis confirmed the previously reported existence of a lamellar morphology and led to a detailed knowledge of the lamellar structural parameters (lamellar long period, crystalline and amorphous layers' thickness etc.). To analyse the data, we employed the pseudo-two-phase model [4], which seems quite appropriate to describe the overall morphology of these iPP-rich blends. Moreover, previous analysis [1,2] led to the conclusion that in the composition range 70–30% w/w in iPP and in the temperature range 90–210°C, iPP/HOCP blends show a miscibility gap leading to the formation of two different coexisting amorphous phases, intercalating between crystalline iPP layers (see Fig. 1).

Our structural investigation in the past has been limited to iPP-rich blends [4]. In fact, the SAXS patterns of *in gap* (HOCP-rich) blends cannot be directly described and interpreted in terms of a pseudo-two-phase model, for reasons which will become clear in the following.

The indication of the occurrence of a phase separation leading to the formation of a novel amorphous phase, with a different composition with respect to the original one has been derived in the past by means of techniques other than SAS, such as differential scanning calorimetry and electron microscopy [1,2]. Moreover, our experimental findings

* Corresponding author. Tel.: + 44-131-449-5111; fax: + 44-131-451-3180.

E-mail addresses: a.triolo@hw.ac.uk (A. Triolo), triolo@unipa.it (R. Triolo).

0032-3861/00/$ - see front matter
PII: S0032-3861(99)00403-6

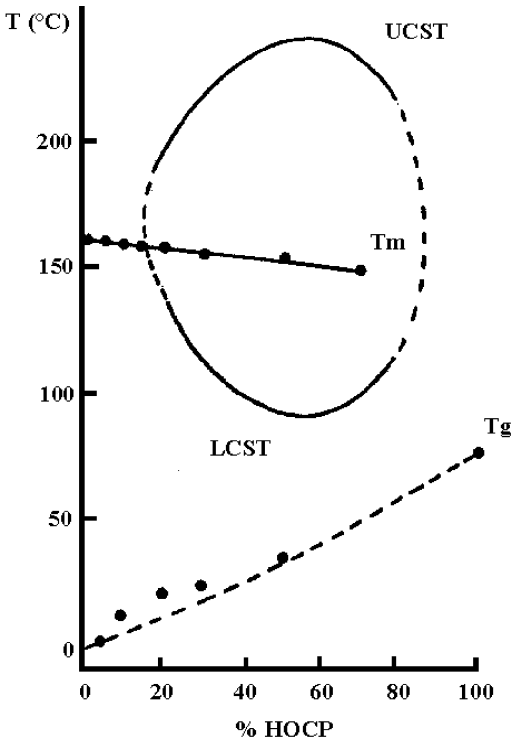

Fig. 1. A schematic representation of the phase diagram of iPP–HOCP binary mixture. This blend presents a miscibility gap, with both an upper and lower consolation points [1,2].

show a peculiar behaviour that can be interpreted in terms of the above-mentioned model. For example, in Fig. 2, we present the temperature dependence of the SAXS invariant, Q_0, for the various blend compositions, which were investigated. As described below, some of the states reported in Fig. 2 correspond to *in gap* blends (i.e. those relative to a iPP content lower than 70% w/w). The invariant Q_0 is defined as

$$Q_0 = \int_0^\infty q^2 I(q)\, \mathrm{d}q$$

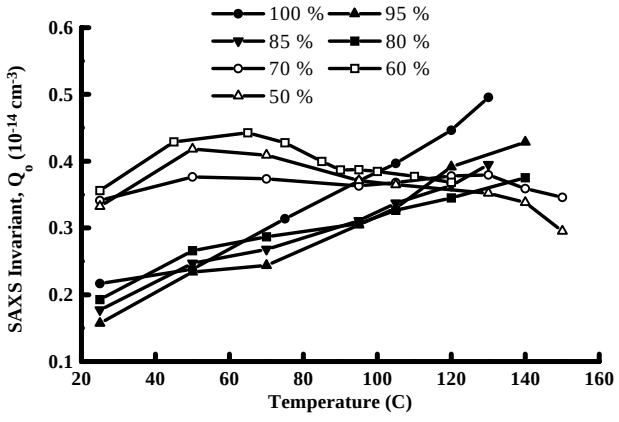

Fig. 2. Temperature dependence of the SAXS derived invariant, Q_0, as obtained for the various compositions (iPP content) that have been investigated.

where q is the scattering momentum vector and $I(q)$ is the measured scattering intensity. In a two-phase system (a semi-crystalline polymer in the solid state can be described as composed of two coexisting phases: the amorphous and crystalline ones), the invariant is related to the amount of scattering matter according to the following relation:

$$Q_0 = \Delta\eta\phi(1 - \phi)$$

where $\Delta\eta$ is the electron density contrast between the two phases and ϕ the fraction of the minority phase (actually the symmetry of this definition with respect to ϕ reflects the so-called Babinet's principle, which states that SAS experiments do not allow characterising a particular phase with respect to the other, but only their contrast).

In Fig. 2, it is evident the occurrence of a master curve describing the temperature dependence of the invariant for iPP-rich blends (*out of gap* blends). On the other hand, a both qualitatively and quantitatively different behaviour can be observed for *in gap* blends (HOCP-rich blends). Moreover, it is evident the occurrence of further changes as soon as the temperature enters the miscibility window (i.e. close to 80–90°C). We do not attempt to quantitatively interpret this behaviour, but it is nevertheless a substantial qualitative confirmation of the occurrence of a structural evolution in the material sample, as the miscibility window is entered.

In order to gain a better understanding of the structural behaviour of *in gap* blends, we also run an extensive set of small-angle neutron scattering (SANS) measurements on these systems. In this case, the use of SANS is somehow unconventional but necessary to investigate the distribution of the additive (HOCP) in the bulk material. We wish to stress this point in order to enhance the SANS-derived information with respect to the one derived from SAXS; as a matter of fact SAXS measurements can be run even on neat iPP (see e.g. Ref. [4]), and a very well defined interference peak would be obtained. This is a consequence of the interference between X-rays scattered from regions, which are characterised by different electron density: the amorphous and crystalline iPP phases. Although these two phases have the very same composition, their bulk densities are so much different that X-rays appreciate a substantial electron density contrast. Whereas this is not the case for neutrons, due to the fact that they are not sensitive to electron density fluctuations; instead they are scattered by the occurrence of the so-called scattering length density fluctuations. As the sum of the coherent scattering length of carbon ($\sigma_{\mathrm{coh,C}} = 6.65 \times 10^{-15}$ m) and twice the contribution from hydrogen ($2\sigma_{\mathrm{coh,H}} = -7.48 \times 10^{-15}$ m) is close to zero, there is almost no contrast with neutrons, and therefore the SANS scattering from neat iPP provides a very poor signal. In contrast, HOCP distributes itself into the amorphous iPP layers and its chemical composition determines a definite contrast between amorphous and crystalline layers, even from the SANS point of view. It is then evident

that in order to characterise the distribution of HOCP inside the amorphous iPP phase, we need to use a probe, which is sensitive to HOCP itself. As described in the following sections, SANS measurements reveal that it seems to be appropriate to describe the *in gap* blends morphology by means of a model of the two coexisting pseudo-two-phase structures. Analysis of SANS patterns thus gains a detailed knowledge of the structural parameters of the two coexisting lamellar structures.

Before describing the experimental work, we briefly outline some of the work that has been performed in literature to analyse SAS data to extract structural parameters of lamellar morphologies.

There are plenty of papers dealing with SAXS data of semi-crystalline polymeric materials which are treated by means of the Fourier inversion (FI) method (see e.g. Refs. [5–10]), firstly introduced by Vonk and Kotleve [11], and successively developed from Strobl and Schneider [12] (the correlation-function approach). We describe this analysis approach in the following sections, but now it is relevant to assess that this approach leads to average structural information (e.g. information on the average crystalline and amorphous layers' sizes, on the long period etc.). This approach has been applied to the SAXS data set that we have reported in our previous paper [4] on the *out of gap* iPP–HOCP blends.

More recently, another analysis approach, the interface distribution function, appeared in literature and it can potentially be even more powerful than the correlation-function approach. This method is due to Ruland and Stribeck (R–S) [13–15] and allows us determining the distribution functions of the various layers' (amorphous, crystalline, long period) thickness present in the material. For a detailed description of the method, we refer the interested reader to the original papers. This approach provides a great deal of information on the nature of the lamellar morphology: in a sense, the correlation-function approach provides an average information, while the R–S one allows us to derive the same information from a powerful statistical point of view.

To our experience, anyway, this last approach is less straightforward to be applied than the Strobl–Schneider one. Moreover, the R–S approach requires a detailed knowledge of the nature of the interface between crystalline and amorphous layers, to be applied. It follows that such an approach is applicable only in well-defined situations, as it requires wide q-range SAS data sets (this is a consequence of the necessity of using the Porod region of the SAS tail). Moreover, in the peculiar case we are currently treating, where a bimodal lamellar morphology is present, the subtraction of a Porod term from the experimental SAS pattern could not be correct, as there is an evidence of the existence of two different interfaces, with different features, between amorphous and crystalline layers. However, for completeness, we cite that bimodal lamellar morphologies have been described in the past by means of the R–S's approach [16], deriving the interface distribution functions.

2. Materials and methods

Our samples are commercial blends of isotactic polypropylene (iPP), Moplen T30S Montedison with $M_w = 3.0 \times 10^5$ and hydrogenated mixture of isomers of cyclopentadiene, Escorez of ESSO Chemical Co., with $M_w = 630$, $T_g = 85 \pm 5$°C and density 1.07 g/cm^3 were used. Although no figure has been given for the polydispersity index, the material has been described as reasonably monodisperse. A small amount (less than 0.2% w/w) of antioxidant was added before making the blends. The blends were prepared by extruding the two components with a twin-extruder at about 280°C. After extrusion, the blends were cooled to room temperature and granulated. The compositions (% w/w) of the iPP–HOCP blends studied were 70:30, 60:40, 50:50, 40:60. The samples, consisting of discs about 1 cm diameter and 1 mm thick, were obtained by melting the granulated blends at about 240°C and then quickly quenching them in H_2O–methanol at −20°C. They were kept at this temperature until ready for measurements.

The data were collected at the W.C. Koehler 30 m SANS facility [17] at Oak Ridge National Laboratory (ORNL) with a 64 × 64 cm^2 position-sensitive proportional area detector of cell size ≈1 cm^2. The neutron wavelength was 4.75 Å ($\Delta\lambda/\lambda \approx 5\%$). The sample-detector distance was 3.21 m and data were corrected for instrumental backgrounds and detector efficiency on a cell-by-cell basis, prior to radial averaging to give a Q-range of $0.0785 < Q < 1.94$ nm^{-1}. The net intensities were converted to an absolute (±4%) differential cross-section per unit sample volume (in units of cm^{-1}) by comparison with secondary standards [18]. The samples were contained in aluminium cells equipped with quartz windows.

In order to account for the incoherent contribution to the scattering, an almost flat background was then subtracted, being $I_{BKG}(q) \approx q^b$, with b varying between 0.06 and 0.2 and determined as a fitting parameter.

SAXS studies were performed with the 10 m SAXS camera of Oak Ridge National Laboratory (USA) [19]. The system uses a three pin-hole collimation configuration, and therefore there is no need for the slit desmearing correction, and is equipped with a 20 × 20 cm^2 two-dimensional (2D) position sensitive detector of 1.0 × 1.0 mm^2 pixel size. The sample-to-detector distance varied between 2 and 5 m (3.12 m for most samples) and CuK_α radiation ($\lambda = 1.54$ Å) produced with the copper rotating anode of a 12 kW Rigaku X-ray generator was used. The samples were contained in stainless steel cells equipped with Kapton windows. The scattered intensity of all the samples was isotropic and the radial averaging was performed on the scattering data that were corrected for electronic noise in the detection system, cosmic radiation background, scattering of the empty sample cell, sample transmission and thickness and the detector uniformity. All the SAXS scattering intensities were converted to an absolute differential cross-section (in cm^{-1}) by means of pre-calibrated secondary standards [20].

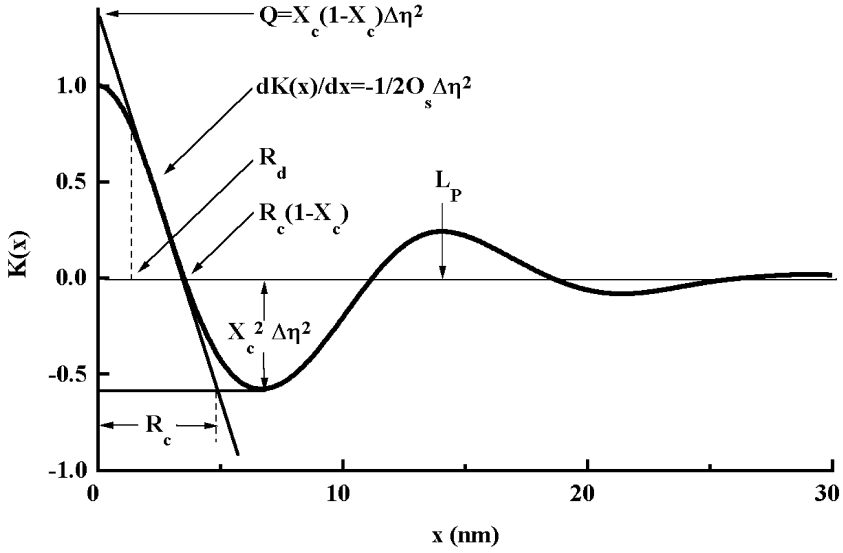

Fig. 3. Experimental electron density correlation function, $K(x)$, obtained for a 95:5 (% w/w) iPP–HOCP blend, at 95°C. The geometrical analysis leading to the direct determination of the structural parameters was implemented in a FORTRAN code [4].

The scattering curve was extrapolated at high q values by means of a power law behaviour of the form $I_{extr} \sim 10^{(aq+b)}$, with value for the a parameter of about 2 nm.

Samples were studied as a function of temperature. In the starting material, the polypropylene crystallises always in the monoclinic α form, [21–23] as evidenced from WAXS measurements [4]. Samples were crystallised isothermally and scattering patterns of several 30 min duration were recorded consecutively at each temperature and summed up until the scattering intensity reaches a constant count-rate. After changing to and stabilising at the desired temperature, the procedure was repeated. Usually it takes a few minutes to reach a thermal equilibrium, as indicated by the tendency to a constant counting-rate.

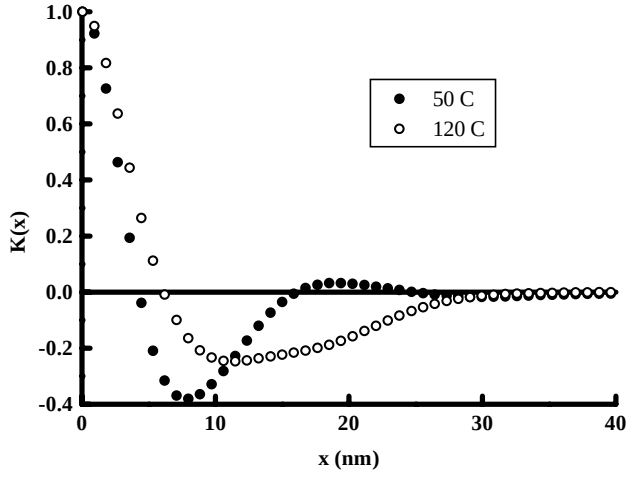

Fig. 4. Comparison between SAXS-derived $K(x)$ as obtained from FI of LC data from a 60:40% w/w iPP–HOCP blend at 50 and 120°C. A substantially different behaviour can be observed as soon as the system material enters the miscibility gap (i.e. at high temperature).

3. Results and discussion

Although in principle the experimental SAS pattern does contain all the information on the lamellar morphology, a more straightforward indication on its structural features can be derived by means of the FI of the Lorentz corrected (LC) patterns of experimental scattering intensity.

This mathematical operation leads to the 1-D electron (as these are the particles which scatter X-rays) density correlation function, $K(x)$:

$$K(x) = \frac{1}{2\pi^2} \int q^2 I(q) \cos(2\pi qx)\, dq.$$

The definition of the correlation function $K(x)$ can alternatively be given in the real space, according to

$$K(x) = \int \rho(x_0)\rho(x_0 - x)\, dx_0$$

where $\rho(x)$ is the electron density function and the integration is run over all the real space. In other words, the $K(x)$ function is related to the probability of finding the electron density to be equal in two different points at a distance of x apart.

We run calculations evaluating the $K(x)$ corresponding to a simulated 1-D lamellar profile. The $K(x)$ maximum appears for those x values corresponding to the average repeat distance, i.e. the Long Period, of the lamellar structure. A careful analysis of the relationship between $\rho(x)$ and $K(x)$ plots leads to the possibility of relating $K(x)$'s geometrical feature to the structural parameters of the lamellar morphology described by the $\rho(x)$ function. A FORTRAN code has been implemented to automatically extract the structural parameters, according to a lamellar model, from the $K(x)$, as obtained from FI of LC SAS data. In Fig. 3, we present the $K(x)$ as calculated from FI of LC SAXS data

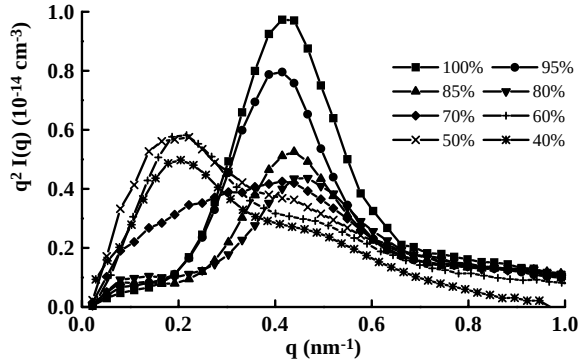

Fig. 5. Lorentz corrected SAXS patterns for a series of iPP–HOCP blends, at 105°C. When the miscibility gap is entered (iPP content lower than 70 (% w/w)) two contributes build up the experimental patterns.

from a 95:5 iPP–HOCP blend at 95°C [4]. In the figure, we also report the structural parameters that can be extracted from the geometrical features of $K(x)$, following Ref. [12]. However, this model cannot be applied further when two different lamellar structures coexist (although existing in different spatial regions of the system material), unless one finds the way to separately evaluate the two $K(x)$s corresponding to the different lamellar morphologies, respectively. For example, in Fig. 4 we show a comparison between the SAXS derived $K(x)$ for the same 60:40% w/w iPP–HOCP, thermally treated at two different temperatures corresponding to states *out of gap* (50°C) and *in gap* (120°C). The wealth of features in $K(x)$ from *in gap* blends is a consequence of a new lamellar phase together with that of the original. Obviously, $K(x)$s showing this behaviour cannot be interpreted and analysed in terms of the pseudo-two-phase model, which, in turn, was applied to the description of the out of gap blends [4] and is commonly applied in such situations. It is quite common to find in literature evidences of this kind of morphologies. For example in Ref. [9], the authors dealt with a semi-crystalline/semi-crystalline PVF_2/PBA polymer blends, which, when the

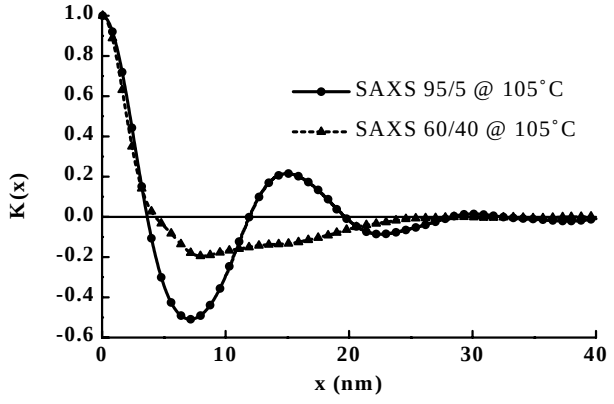

Fig. 6. Comparison between $K(x)$, as derived from SAXS patterns of 95:5 and 60:40 (% w/w) iPP–HOCP blends at 105°C, respectively. *In gap* blends show a $K(x)$ which cannot be described by means of the pseudo-two-phase model.

two components were in the crystalline phase, showed two SAXS peaks, each corresponding to the different lamellar domains. The $K(x)$s features were presumably similar to the ones that we currently observe in our data set (the authors do not present these plots) and the authors did not develop an analysis approach to account for this behaviour. Actually, as we anticipated in the introduction, apart from the work of Stribeck [16], to our knowledge, no detailed analysis has been ever made to this kind of systems where two different morphologies are coexisting. Moreover, in such situations, the correct subtraction that the interfaces contribute (which is a fundamental step of Stribeck approach) cannot be ensured, as two different interfaces are simultaneously present, building up this contribution.

We, therefore, tried to develop an analysis approach which could allow the distinction between the different components to $K(x)$, when dealing with demixed systems.

In Section 1, we already noted that SAXS experiments are a sensitive probe to evidence a coexistence of the two different lamellar domains in the phase-separated blends. In Fig. 5, we show the composition dependence of the SAXS patterns, as obtained from blends thermally treated at 105°C. For blends containing an HOCP content higher than 30% by weight, this temperature defines a thermodynamically phase separated state. The experimentally obtained SAXS patterns, $I(q)$, were corrected by multiplying with the Lorentz factor (i.e. the term q^2, q is the momentum transfer), which accounts for the lamellar arrangements of the scattering matter.

Out of gap blends show a quite common SAXS pattern: only a well-defined peak appears, whose presence is due to the constructive interference between radiation diffused by matters arranged in a lamellar fashion.

On the other hand, as soon as the miscibility window is entered (i.e. as the HOCP content amounts to 30% by weight or more), a second peak appears at lower q values, while the first peak position remains practically unaltered. This peak is the consequence of the constructive interference between radiation diffused by the newly appeared lamellar domains.

This observation is thus indicative of the appearance of a new lamellar phase as soon as the miscibility window is entered. The same kind of indication can be obviously derived from the $K(x)$ analysis, as it must reflect, in the x-domain, the behaviour observed in the q-domain. In Fig. 6, we show a comparison from $K(x)$s as obtained from FI of LC SAXS patterns from two blends lying out of the miscibility gap (the 95:5 at 105°C) and inside (the 60:40 at 105°C), respectively.

It is evident that the $K(x)$ corresponding to the *in gap* blend show geometrical features that make it completely different from the *out of gap* blend; while iPP-rich (e.g. the 95:5) blends show a SAXS pattern which can be straightforwardly interpreted by means of the pseudo-two-phase model, the SAXS patterns from iPP-poor (e.g. the 60:40) blends show a complex behaviour and lack sharp

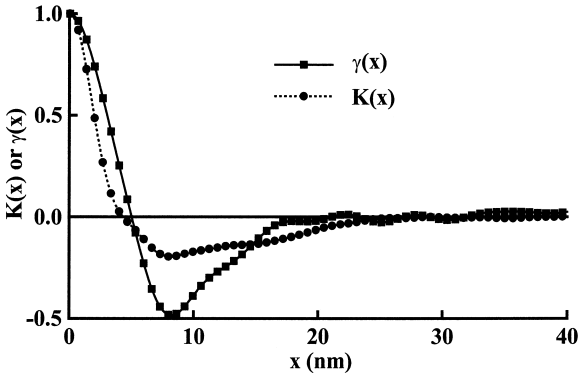

Fig. 7. Comparison between SAXS-derived $K(x)$ and SANS-derived $\gamma(x)$ for the very same 60:40 (% w/w) iPP–HOCP sample, at 105°C. The SANS derived $\gamma(x)$ can be described as a combination of two *out of gap* $\gamma(x)$.

geometrical features to be readily related to structural parameters.

If, on the one hand, SAXS thus reveals its capacity to detect the peculiar transformation occurring in the sample material as the phase separation occurs (both in q- and in x-domains), on the other hand, it shows a wealth of details that, in a sense, covers the main information. For example, it is not clear whether the origin of the newly formed interference peak depends only on the formation of the new lamellar domains, or, in turn, if a contribution from higher order diffraction peaks is present (the SAXS signal corresponding to twice the thickness of the long period should fall very close to the position of the new peak).

A strong confirmation of this SAXS over-wealth can be seen in Fig. 7, where we show a comparison between the $K(x)$ obtained from FI of SAXS data from a 60:40% w/w iPP–HOCP blend at 105°C and the one, hereinafter called $\gamma(x)$, obtained from FI of SANS data from the same material (we note, by passing, that no isotopic substitution was

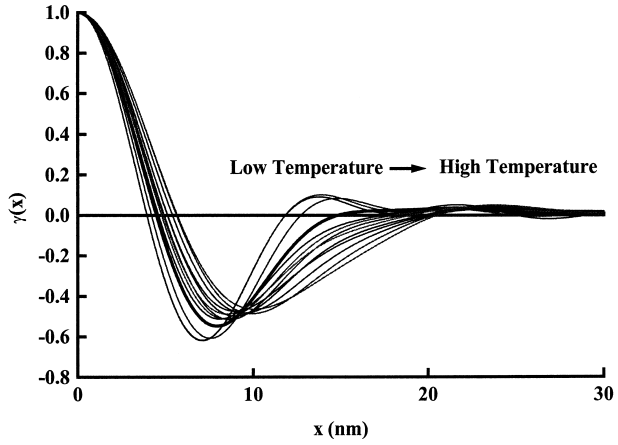

Fig. 8. SANS derived $\gamma(x)$ for 40:60 (% w/w) iPP–HOCP blend as a function of temperature. It appears that, as the miscibility gap is entered, a secondary minimum appears at ca. 15 nm, as a consequence of the occurrence of a new kind of lamellar mesodomain with a different periodicity: the heavy line curve corresponds to 90°C, which is the temperature at which our analysis indicates the miscibility gap boundary.

necessary in order to observe measurable SANS patterns, as the addition of HOCP created sufficient natural scattering contrast for neutrons).

It can be argued from Fig. 7 that the experimental $\gamma(x)$ can be interpreted as obtained from a combination of two $\gamma(x)$s, each related to one of the two coexisting lamellar morphologies, while on the contrary, it is less obvious to derive the same indication from the $K(x)$ function, as SAXS patterns show more complicate features than SANS.

In Fig. 8, we show the temperature dependence of $\gamma(x)$ as obtained from the FI of LC SANS patterns for the 40:60% w/w iPP–HOCP composition. It is quite evident that the occurrence of the phase separation transition at $T \approx 90$°C corresponds to the appearance of a secondary minimum at $x \sim 15$ nm in the $\gamma(x)$. This is an indication that the structural transition (i.e. the formation of the new lamellar domains) occurs as soon as the miscibility gap is entered.

Up till now, only qualitative description of blends' morphology was outlined. In order to get quantitative structural details by means of the application of a pseudo-two-phase model, we formulated the hypothesis that the two coexisting lamellar morphologies are independent and thus uncorrelated. In other words, the two kind of lamellar mesodomains are far apart enough not to influence each other. Then, the scattered intensity from a phase separated material system can be interpreted as a linear combination of independent contributions from the two kinds of mesodomains. Accordingly the LC SANS pattern can be described by a combination of two independent contributions, each described by means of a Gaussian function. The LC experimental patterns have been fitted with one or two Gaussian functions (according to the existence of just one or two kinds of mesodomains), so that we had

$$q^2 I_{\mathrm{cor}}(q) = A_1 \exp\left(\frac{(q-q_1)^2}{2c_1^2}\right) + A_2 \exp\left(-\frac{(q-q_2)^2}{2c_2^2}\right)$$

where $I_{\mathrm{cor}}(q)$ is the corrected experimental SANS intensity, q_i, c_i and A_i, are the centre, the variance and the amplitude of the i-th Gaussian function, respectively. Fig. 9(a), shows the result of a typical fit. It is noted that in passing for all the materials studied, fits of similar quality were achieved.

Evidently, each Gaussian function represents the interference peak originating from each kind of a lamellar mesodomain. In this situation, we have decomposed the problem of dealing with a SAS pattern containing two contributes, each coming from a different lamellar domain, into a fairly simple problem of dealing with two SAS patterns, each containing structural information on a single lamellar domain. Therefore, with the FI of these single contributes to the SAS pattern, we derive the $\gamma(x)$ functions representing the self correlation functions of the scattering length (as we mentioned earlier, in SANS, neutrons are not scattered anymore by electronic density fluctuations, but

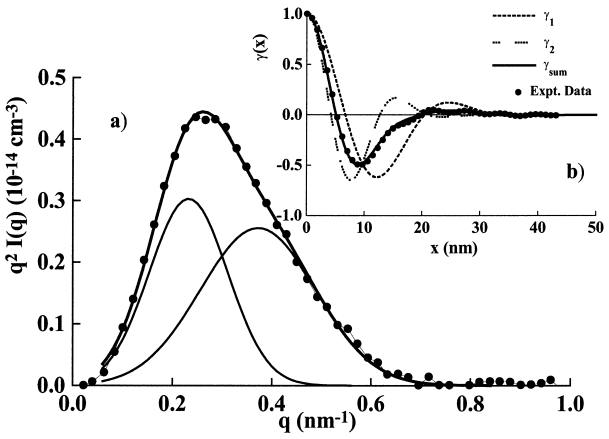

Fig. 9. (a) LC SANS pattern from 60:40 (% w/w) iPP–HOCP blend at 105°C. Experimental data are fitted with two Gaussian functions (see text for details). (b) Results of the Fourier inversion of LC SANS data and of the Gaussian functions as reported in (a).

only from scattering length) of the two lamellar morphologies; and these $\gamma(x)$s are termed $\gamma_1(x)$ and $\gamma_2(x)$.

In Fig. 9(b), we compare the experimental $\gamma(x)$, as derived from FI of LC SANS pattern with the weighted sum of $\gamma_1(x)$ and $\gamma_2(x)$, $\gamma_{sum}(x)$ for the case of the 60:40% w/w iPP–HOCP blend thermally treated at 105°C.

It should now be noticed that $\gamma_1(x)$ and $\gamma_2(x)$ possess the same geometrical features that were found for blends lying outside the miscibility gap. In other words, our approach has successfully separated the two distinct contributes to experimental $\gamma(x)$, arising from the two coexisting lamellar morphologies.

The simple geometric approach that was previously applied to the *out of gap* blends can now be applied to the single self correlation functions $\gamma_1(x)$ and $\gamma_2(x)$, so that each of $\gamma_1(x)$ and $\gamma_2(x)$ (for each SANS measurement) will be interpreted by means of the approach reported in Fig. 3.

This analysis allows deriving a better knowledge of the structural parameters of the two lamellar structures. In our analysis, we refrained from studying the tail of the scattering curve to derive information on the nature of the transition layer between amorphous and crystalline layers, as both the limited q range investigated and the overlapping of tails from the two kinds of lamellar structure make it difficult to arrive at any conclusive interpretations. Moreover, the description of the scattering from a domain in terms of a Gaussian curve does not allow any analysis of the high q portion of the curve in terms of an interface contribution (i.e. the high q portion of a Gaussian does not follow the Porod behaviour ($I(q) \sim C/q^4$)).

Fig. 10 presents the temperature evolution for the structural parameters of the 40:60% w/w iPP–HOCP blend. It appears that up to 90°C, only a structural contribution is present; later at 93°C, we found it necessary to introduce the existence of a new scattering contribute at low Q values. Applying the aforementioned data analysis approach, we obtained the scattering from the two domains and the corresponding lamellar parameters, as reported in Fig. 10. It is interesting to note that our results are in good agreement with the blend phase diagram, which was obtained by means of different techniques other than SAS [1,2], and a detailed description of the miscibility gap boundary was obtained by means of SANS technique (i.e. characterisation of the demixing temperature, which was later found to be between

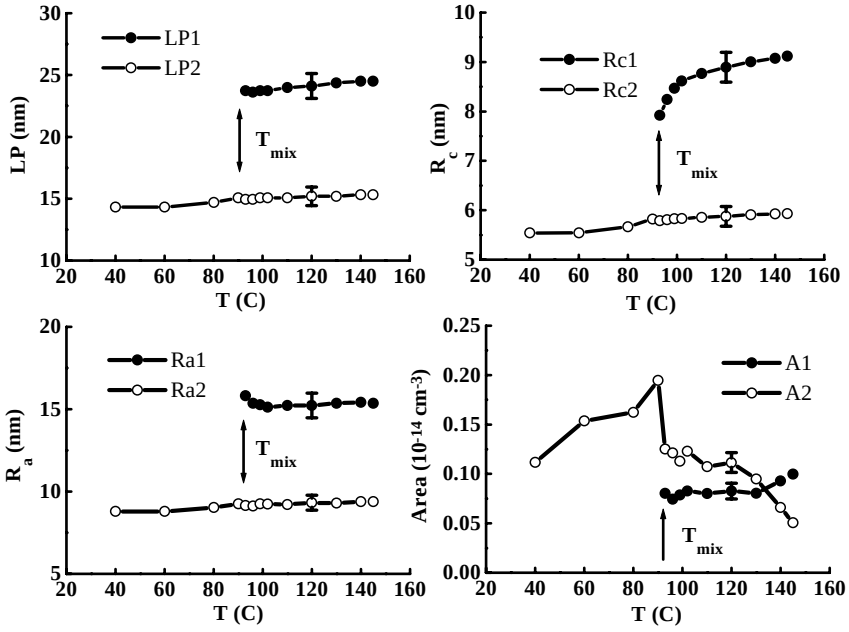

Fig. 10. Temperature dependence of Long Period, crystalline and amorphous layers' thicknesses and of the fitting Gaussian functions areas (see text for details) for the 40:60% w/w iPP–HOCP blend. Typical error bars are reported for $T = 120$°C. The demixing temperature, T_{mix}, as obtained from the fitting procedure is indicated in each plot.

90 and 93°C). Regarding the other blend compositions, similar temperature evolutions were obtained inside the miscibility gap. However, we were unable to run the same detailed temperature grid as for the 40:60 sample, hence we could not characterise the phase boundary in the same manner.

In Fig. 10, we also present some geometrical parameters related to the two Gaussians building up the LC SANS peak, for the 40:60 blend. In particular, the area underlying these curves, hereinafter indicated as $Q_{0,i}$, i is the index referring to the i-th Gaussian, is reported as a function of temperature. It can be easily understood that this parameter is related to the invariant that has been previously introduced. A strong decrease of $Q_{0,1}$ can be observed as the miscibility gap is entered, as a consequence of the sharing of the scattering matter in two different domains, thus building up the two contributes to Q_0, $Q_{0,1}$ and $Q_{0,2}$. These two terms are almost similar in magnitude, thus being a consequence of the symmetry of the miscibility gap boundary around the 40:60% w/w iPP–HOCP composition, assuming that there is no large difference in the contrast in the two domains (see for definition of invariant in Section 1).

A very limited temperature dependence of the structural parameters (e.g. LP, R_c or R_a) can be observed, especially if referred to the same evolution in the iPP-rich blends, as obtained from the SAXS characterisation [4]. However, this limited temperature dependence is observed also at temperature below the demixing one (i.e. 93°C for 40:60 blend), and it is an indication that this is a real physical effect and not a mere artefact of the analysis approach we propose in this work. Presently, we have not found a rationalisation for this evidence, but it should be related to the large HOCP content in the blend.

4. Conclusions

In this report, we present SAXS and SANS patterns from iPP–HOCP blends. Varying composition and temperature ranges were chosen in order to investigate blend structural features in a region of the phase diagram leading to the coexistence of two different lamellar mesodomains.

The SAS patterns were analysed by means of a pseudo-two-phase model after FI of corrected scattering data. The experimental SAXS data appear to be difficult to treat by means of this approach. On the other hand, the SANS patterns by FI show geometrical features that can be directly related to the coexistence of two different lamellar mesodomains.

In order to gain information on the structural parameters of the two kinds of lamellar stacks, we presented a novel analysis approach to extract the contributes to LC SANS patterns arising from the two different lamellar mesodomains. The two corresponding self-correlation functions, $\gamma_i(x)$s, have been obtained by FI of the two Gaussian functions fitting LC SANS patterns. Application of a well established geometrical construction (i.e. the pseudo-two-phase model) to each of the two $\gamma_i(x)$s allows deriving a detailed knowledge of structural parameters of the two lamellar mesodomains. The analysis of the results obtained from 40:60% w/w iPP–HOCP blend allowed a detailed characterisation of the miscibility gap phase boundary (between 90 and 93°C), and showed a limited temperature dependence of the lamellar parameters.

Acknowledgements

The research was supported in part by the Italian Ministero dell'Universita'e della Ricerca Scientifica (MURST) and the Italian National Research Council (CNR) and in part by the Division of Material Sciences, U.S. Department of Energy under contract number DE-AC05-96OR22464 with Lockheed Martin Marietta Energy Research Corporation. A.T. acknowledges a research scholarship granted by CNR.

References

[1] Cimmino S, Di Pace E, Karasz FE, Martuscelli E, Silvestre C. Polymer 1993;34:972.
[2] Cimmino S, Martuscelli E, Silvestre C. Macromol Symp 1994;78:115.
[3] Caponetti E, Chillura Martino D, Cimmino S, Floriano MA, Martuscelli E, Silvestre C, Triolo R. J Molec Struct 1996;383:75.
[4] Triolo A, Silvestre C, Cimmino S, Martuscelli E, Caponetti E, Triolo R. Polymer 1998;39:1697.
[5] Ryan A, Stanford JL, Bras W, Nye TMW. Polymer 1997;38:759.
[6] Myers ME, Wims AM, Ellis TS, Barnes J. Macromolecules 1990;23:2807.
[7] Silvestre C, Karasz FE, MacKnight WJ, Martuscelli E. Eur Polym J 1987;23:745.
[8] Schmidtke J, Strobl G, Thurn-Albrecht T. Macromolecules 1997;30:5804.
[9] Liu LZ, Chu B, Penning JP, Manley RStJ. Macromolecules 1997;30:4398.
[10] Wilson Cheung Y, Stein R, Lin JS, Wignall GD. Macromolecules 1994;27:2520.
[11] Vonk CG, Kortleve G. Kolloid-Z und Z Polymere 1967;220:19.
[12] Strobl GR, Schneider M. J Polym Sci: Polym Phys Ed 1980; 18:1343.
[13] Ruland W. Colloid Polym Sci 1977;255:417.
[14] Stribeck N, Ruland W. J Appl Cryst 1978;11:535.
[15] Stribeck N. J de Phys IV 1993;C8:507.
[16] Sribeck N, Alamo RG, Mandelkern L, Zachmann HG. Macromolecules 1995;28:5029.
[17] Koehler WC. Physica (Utrecht) 1986;137B:320.
[18] Wignall GD, Bates FS. J Appl Cryst 1986;20:28.
[19] Wignall GD, Lin JS, Spooner S. J Appl Cryst 1990;23:241.
[20] Russell TP, Lin JS, Spooner S, Wignall GD. J Appl Cryst 1988;21:629.
[21] Vittoria V, Riva F. Macromolecules 1975;19:1986.
[22] Natta G, Peraldo M, Corradini P. Rend Acc Naz Lincei 1959; 26:14.
[23] Fichera A, Zanetti R. Macromol Chem 1975;176:1885.